water

Article

Comparison of the Causes of Erosion-Deposition between Yellow River, Yangtze River and Mekong River Subaqueous Deltas II: Comparative Analysis

Bowen Li [1,*], J. Paul Liu [2] and Yonggang Jia [3,4]

1 College of Oceanography and Space Information, China University of Petroleum, Qingdao 266580, China
2 Department of Marine, Earth and Atmospheric Sciences, North Carolina State University, Raleigh, NC 27695, USA
3 Laboratory for Marine Geology, Qingdao National Laboratory for Marine Science and Technology, Qingdao 266100, China
4 Shandong Provincial Key Laboratory of Marine Environment and Geological Engineering, Ocean University of China, Qingdao 266100, China
* Correspondence: 20200111@upc.edu.cn

Abstract: The estuary delta is an area where human economic activities are active and natural ecological environment is fragile. With global change and the intensification of human activities, coastal and seabed erosion around the world is becoming more and more serious. In this paper, we used the Delft 3D numerical simulation to compare the hydrodynamic effects of sediment transport paths in the Yellow River delta (river-controlled type), Yangtze River delta (tidal type) and Mekong River delta (tidal wave type) in the East Asian monsoon area, and analyzed the causes of accumulation erosion landform distribution in three different types of subaqueous deltas. This study finds the Yellow River Delta has experienced varying degrees of erosion at the estuary, but its subaqueous delta is still dominated by deposition; the Yangtze River Delta has ensured the stability of its shoreline under the influence of artificial shoreline reinforcement, but the subaqueous delta (water depth: 0–15 m) is in a state of erosion all year round; and in the Mekong River Delta the erosion occurs in both its shoreline and subaqueous delta. Additionally, only by analyzing the erosion and deposition within the transport range of resuspended sediment, the changes in the properties of the entire subaqueous delta could be recognized. The research results can not only be helpful to analyze whether the change of river sediment will lead to the change of delta type under human influence, but also provide more powerful scientific support for the protection of delta ecological environment, geological environment safety and geological disaster prevention.

Keywords: hydrodynamics; sediment resuspension; sediment transport; erosion–deposition; deltas in East Asia monsoon area

check for updates

Citation: Li, B.; Liu, J.P.; Jia, Y. Comparison of the Causes of Erosion-Deposition between Yellow River, Yangtze River and Mekong River Subaqueous Deltas II: Comparative Analysis. *Water* **2023**, *15*, 38. https://doi.org/10.3390/w15010038

Academic Editor: Bommanna Krishnappan

Received: 28 October 2022
Revised: 15 December 2022
Accepted: 20 December 2022
Published: 22 December 2022

1. Introduction

Since the 1950s, due to the influence of human activities including reservoirs and dams, the amount of sediment transported by large rivers in East Asia, such as the Yellow River, the Yangtze River and the Mekong River, has decreased significantly [1–4]. Erosion and deposition processes are major environmental degradation threats [5], as water-induced sediment erosion may lead to land degradation [6]. For example, from 2009 to 2018, the Yellow River transported less than 6% of its suspended silt during 1999–2008 [1]. Due to the changes in the amount of suspended sediment transported by the Yellow River in the past 70 years. The geomorphic evolution in the subaqueous delta of the Yellow River has experienced three different stages: rapid accumulation, moderate accumulation and slow accumulation [7]. Additionally, during 2013 and 2015, in the Yangtze River subaqueous delta, the amounts have decreased to 1.20×10^8 tons, which is less than 1/5 of the amount in 1964. However, if the balance between erosion and deposition is reached in the Yangtze

River Delta, the extra amount of sediment needs is at least 6.0×10^8 tons [8]. All this has led to erosion of the Yangtze channel in the estuary and sandbanks. The subaqueous delta of the Yangtze River is also subject to erosion [9].

In addition to the Yellow River and Yangtze River, the Mekong River runoff and sediment fluxes have undergone significant changes due to natural processes and human activities. From 2012 to 2015, the sediment flux of Mekong River was only 43.1×10^6 t/a, less than 30% of the sediment transport before 1992 [2]. As a result, after the completion of the dams, there was almost no river sediment accumulation in the Mekong subaqueous delta [10]. The seabed is subjected to strong shear stress under the action of monsoon [11], which leads to the coastline growth of the Mekong Delta gradually decreasing from 7.8 m/a to 2.8 m/a during 1973 and 2005, and the net land area growth of the Mekong Delta is also slowing down. The average growth rate decreases from 4.3 km^2/a (1973–1979) to 1.0 km^2/a (1995–2005) and then to -0.05 km^2/a (2005–2015) [12]. As a result, the Mekong Delta changed from a constructive delta to an erosive delta around 2005. In addition, the Mekong Delta is gradually reduced, but its subaqueous delta is also gradually eroded, along with the formation of scour trough [12].

On the coastline of CùLaoDung Island, the mangroves growing on muddy sediments are constantly being eroded. It is believed that the sediments transported by rivers are deposited in the intertidal zone, which could prevent some areas from being submerged due to rising sea levels. However, the suspended sediment in this mangrove area is mainly produced by the erosion of the bottom bed caused by hydrodynamic forces [13], due to the suspended sediment transport is mainly concentrated in the dry season when the river effect is small [14]. Therefore, the erosion rate of the southwest coastline was closely related to the strength of hydrodynamic forces. When the wave reached the edge of the mangrove forest, the tidal current rotates vertically from the shore parallel to the shoreline under the combined action of friction, wind and hydrodynamic forces [15]. At the same time, the increase in the drag coefficient also caused the wave to dissipate faster. The wave height only was halved after the wave spreads for tens of meters on the normal beach surface, while in the mangroves, the wave height was halved after spreads for 1 m [16].

In deltas adjacent to bays, the late transformation of sediments [17] and deltaic sedimentary features, including beach erosion, topography and shoreline evolution [18], are influenced by ocean dynamics. The erosion and deposition of subaqueous deltas are caused by the combined action of suspended sediment deposition and hydrodynamic erosion [19]. Wind is the most important driving force of wave and current, and it can be an important factor affecting the direction and distance of sediment diffusion transported by river [20]. Therefore, as one of the driving forces of sediment transport, wind is necessary to analyze the effect of different seasons and wind direction on sediment transport affected by monsoon [21].

In summary, there are different erosion and deposition control factors in the same East Asian monsoon area. Tree rivers have the same source—Himalaya mountains, but with different subaqueous deltas– the Yellow River is river controlled type, the Yangtze River is tidal controlled type, and the Mekong River is tidal wave dominated types. However, as a typical East Asian delta, the amount of runoff and sediment fluxes is significantly decreased due to human activities, which leads to different degrees of erosion in these deltas [22–24]. Although previous studies have identified the distribution characteristics of erosion and deposition landforms in three subaqueous deltas, the mechanism of their formation has received little attention. The type of river delta may change as the amount of sediment fluxes decreases.

For example, according to the observation data of the amount of the runoff and sediment transported by the Yellow River after 2017, the discharge and the suspended sediment concentration (SSC) at the mouth of the Yellow River has decreased significantly under the influence of human factors, and the SSC had dropped below 1 g/L (data from the Yellow River Sediment Bulletin), which is close to the Yangtze River and the Mekong River [25,26]. The sediment amount transported by the Yangtze River still have a significant impact on delta accumulation [27] due to the large discharge with an annual runoff exceeding 9×10^{11} m^3 [25]. However, the SSC of the Yellow River is similar to that of the Mekong River, but the amount of runoff is much smaller than that of the Mekong River, and both are affected by the monsoon climate and the runoff is mostly concentrated in the flood season [26]. Will this suggest that the Yellow River Delta change to a delta dominated by hydrodynamics similar to the Mekong River [28]? This requires further research to predict and confirm. In addition, satellites cannot obtain the erosion and accumulation of subaqueous deltas unlike coastline changes, but they can obtain data such as offshore waves, wind speed and direction. Combining it with the runoff and sediment fluxes obtained by the hydrological station through numerical simulation, the erosion and accumulation situation of the subaqueous delta can be obtained. Therefore, this paper aims to analyze the combined effects of sediment transport and hydrodynamic dynamics in the East Asian estuarine deltas, including the Yellow River Delta (river control type), the Yangtze River delta (tidal river type) [29] and the Mekong River delta (tidal wave type) [30,31] through simulation techniques to determine the formation mechanism and controlling factors of erosion and deposition landforms in three major estuarine deltas in East Asia. Over 3 deltas, tide is dominant or very important in the Yangtze and in the Mekong deltas, so tide-induced currents are a major factor of sediment dynamics. The research results can not only further deepen the understanding of the physical process and mechanism of the erosion and deposition of the subaqueous delta, but also provide more powerful scientific support for the protection of the ecological environment, the safety of the geological environment and the geological disaster prevention of the delta. It also lays the foundation for rapid access to erosion and deposition conditions in subaqueous deltas.

2. Methods

The Delft 3D software and model was used to simulate the sediment transport and the shear stress on the bottom bed during the flood and dry seasons in the Yellow River, Yangtze River and Mekong River subaqueous delta [32]. The Delft 3D software and model is introduced and verified in the paper "Comparison of the Causes of Erosion-deposition between Yellow River, Yangtze River and Mekong River subaqueous delta I: model building" [32].

The average value of the runoff and sediment fluxes in the flood season of the total 7 stations in August and September and the dry season in February and March, 2018 (Table 1, data from the Mekong River Commission) [33] are used as variables for the water-sediment transport process and the shear stress of the bottom bed simulated by Delft 3D in the two seasons of flood and dry season in the Mekong River delta. The Delft 3D software is a mature numerical simulation software, and its model has been verified to simulate sediment dispersal in underwater deltas [32]. The discharge of the each of the 7 stations is 1/7 of the average water flux in Table 1. Because of the flow going back and forth in Mekong estuaries under the tidal effect, the 7 upstream stations are indicated in Figure 1a of the boundary in the branch of the Mekong River (Figure 1a). The tidal is imposed by the software "openearth" considered the lunar semidiurnal tide (M2), lunar diurnal tide (O1), solar semidiurnal tide (S2) and solar diurnal tide (P1). Additionally, the water and sediments cannot go upward at the upper boundary. The mean grain size of the sediment is 24 μm. The average dry bulk density in the top layer of the proximal clinoform yielded is 0.95 g/cm^3 in the Mekong River subaqueous delta [10], and sediments around the Ca Mau Peninsula showed an average dry bulk density of 1.2 g/cm^3 [34]. In this study, we used 1.1 g/cm^3 as a dry bulk density to simulate the suspended sediment transport. The critical shear stress is about 0.20 Pa. The settling velocity is calculated by Stokes settlement formula based on the median diameter and density of sediment in the model.

Table 1. Average values of water, sediment fluxes and wind velocity in the Mekong River during the flood and dry season in 2018.

	Flood Season (July, August)	Dry Season (February, March)
Average water flux	36,000 m^3/s	2500 m^3/s
Average suspended sediment concentration	0.4 g/L	0.2 g/L
Wind velocity	5.0 m/s	7.0 m/s
Wind direction	225°	45°

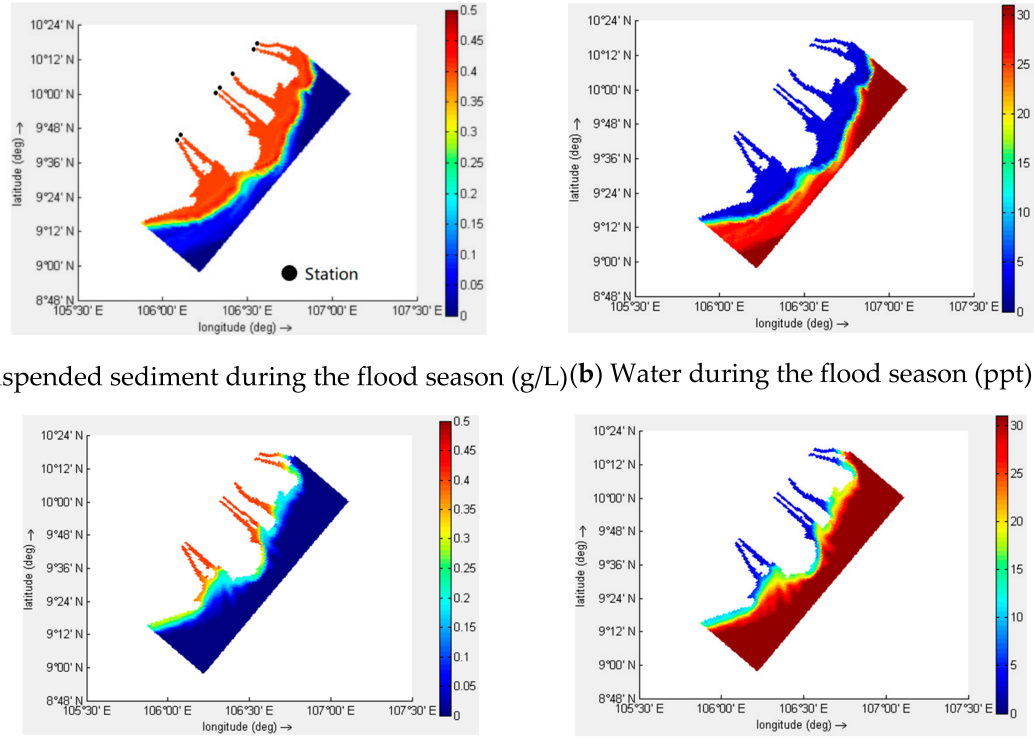

(**a**) Suspended sediment during the flood season (g/L) (**b**) Water during the flood season (ppt)

(**c**) Suspended sediment during the dry season (g/L) (**d**) Water during the dry season (ppt)

Figure 1. The transport of suspended sediment (**a**,**c**) and water (**b**,**d**) in the Mekong River Delta during the flood (**a**,**b**) and dry scheme 2018.

3. Result and Discussion

3.1. The Transport Simulation Results of Water and Sediment in Mekong River Subaqueous Delta

The simulation results show that the seasonal water and sediment transported by Mekong River have a significant impact on the process of water and sediment transport (Figure 1). During the flood season, the flux of sediment entering the sea is relatively larger, and the sediment from the seven estuaries is integrated and spread to offshore. In the dry season, the water and sediment are mainly gathers near each estuary with the fluxes decreases. Based on the coastline, they transport to landward under the tidal effect (Figure 1c).

The transport of water and sediment transported by Mekong River is simulated under the conditions of no wind, east wind, north wind, west wind, south wind in summer, and northerly wind in winter. The simulation results show that under the conditions of no wind in summer, the water and sediment entering the sea from the seven estuaries are connected and transported to the southwest. The most typical character is the formation of a low salt and high suspended sediment concentration area outside the estuary. The area may be created by the mixing of waves and tides (Figures 2a and 3a).

Under the action of the northeast wind in summer, the transportation of sediment to the southwest is obvious. The water and sediment transported by Mekong River are mainly gather in the estuaries, and the spread area to the northeast decrease (Figures 2b and 3b). Under the effect of the northwest wind in summer, the sediment and water transport to the southwest is weaker than that under the northeast wind, and the transport range is correspondingly reduced, while the offshore transport to the southeast increase (Figures 2c and 3c).

Under the conditions of the southwest wind, the sediment and water transport to the southwest is weakened, and the offshore transportation to the northeast and southeast is enhanced (Figures 2d and 3d). Under the southeast wind, the transport of the suspended sediment shows a "compression" trend toward the northwest estuary (Figures 2e and 3e).

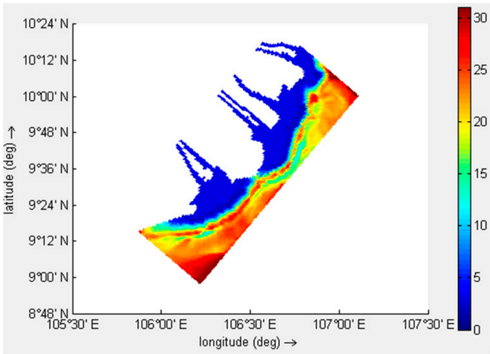

(**a**) No wind in Summer

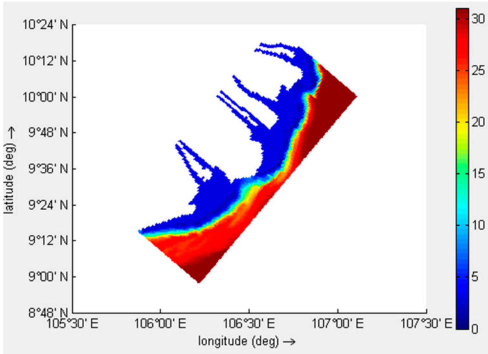

(**b**) Northeast wind in summer

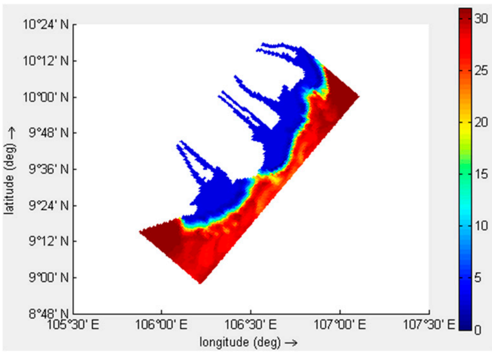

(**c**) Northwest wind in summer

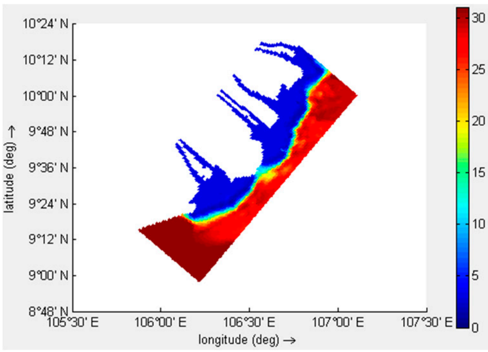

(**d**) Southwest wind in summer

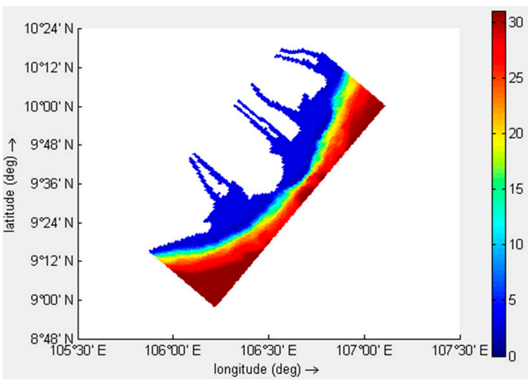

(**e**) Southeast wind in summer

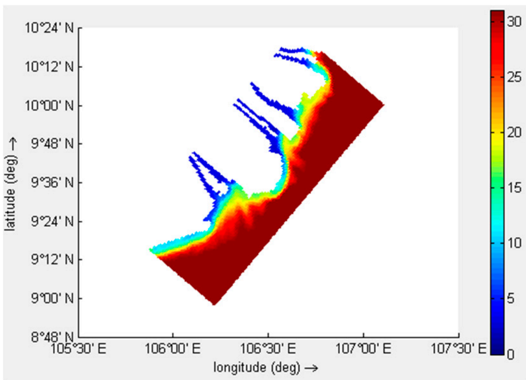

(**f**) Northeast wind in Winter

Figure 2. Water transport at the Mekong River Delta under no wind (**a**), northeast wind (**b**), northwest wind (**c**), southwest wind (**d**), southeast wind (**e**) in summer and northeast wind (**f**) in winter (Unit:ppt).

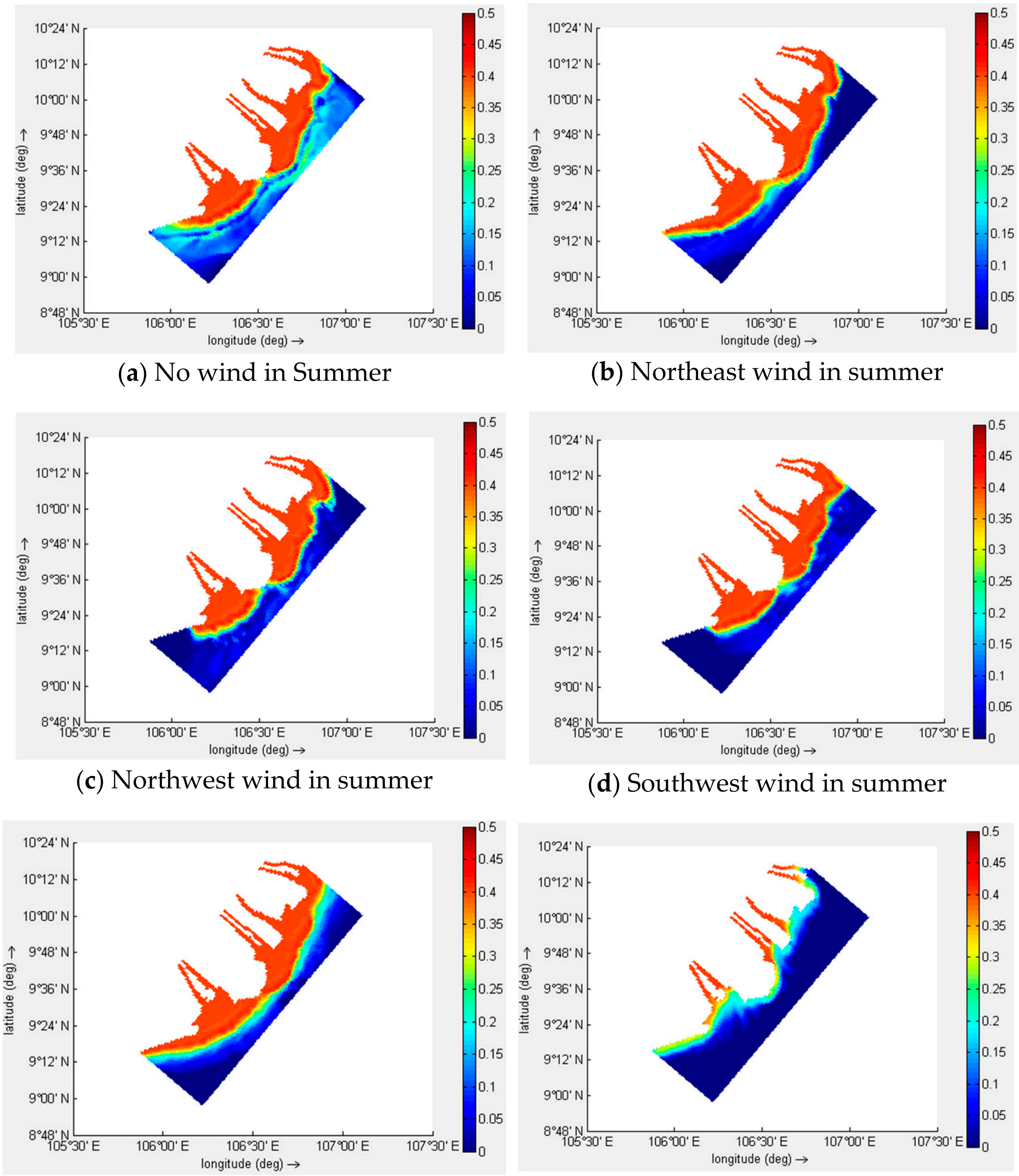

(**a**) No wind in Summer (**b**) Northeast wind in summer

(**c**) Northwest wind in summer (**d**) Southwest wind in summer

(**e**) Southeast wind in summer (**f**) Northeast wind in Winter

Figure 3. Suspended sediment transport at the Mekong River Delta under no wind (**a**), northeast wind (**b**), northwest wind (**c**), southwest wind (**d**), southeast wind (**e**) in summer and northeast wind (**f**) in winter (Unit: g/L).

This illustrates that the transport of the water and sediment is mainly controlled by the wind direction. As the Mekong estuary is affected by the monsoon, it is dominated by the southwest monsoon in summer, and the sediment spreads northeastward along the coast. The northeast monsoon prevails in winter, the wind direction is benefit to transport of water and sediment. However, because of the amount of sediment transported by Mekong River in winter is much less than that in summer and the water is less than 1/6 of that in summer, the transport range of water and sediment discharge in winter is much smaller than in summer, mainly concentrated near the estuaries (Figures 2f and 3f).

3.2. Simulation Results of Shear Stress on the Bottom Bed of the Mekong River Subaquepus Delta

The changes in the shear stress on the bottom bed is simulated in Mekong River subaqueous delta under the conditions of no wind, east wind, north wind, west wind, south wind in summer, and north wind in winter (Figure 4). The simulation results show that under the condition of a certain wind speed, the shear stress on the bottom bed under the action of easterly wind (Figure 4b,e) is greater than that under no wind (Figure 4a) and west wind (Figure 4c,d). Under the northeast wind in winter, the shear stress on the bottom bed is similar to that in the northeast in summer. It indicates the change of wind direction has a greater impact on the shear stress on the bed in Mekong River subaqueous delta.

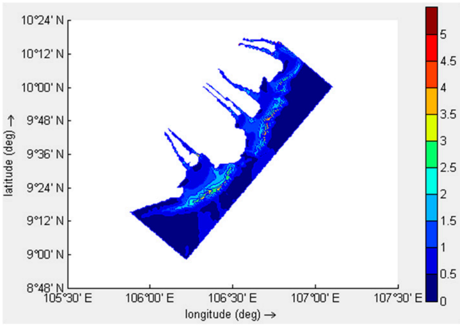

(**a**) No wind in Summer

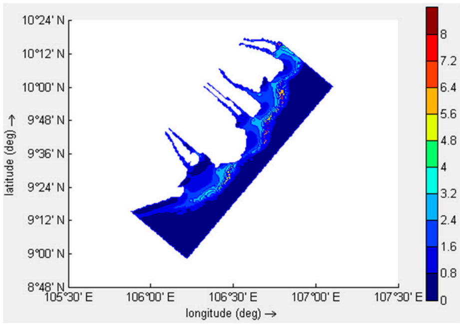

(**b**) Northeast wind in summer

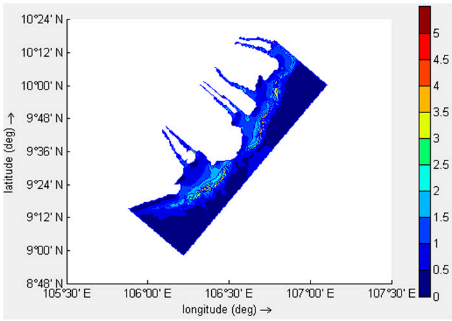

(**c**) Northwest wind in summer

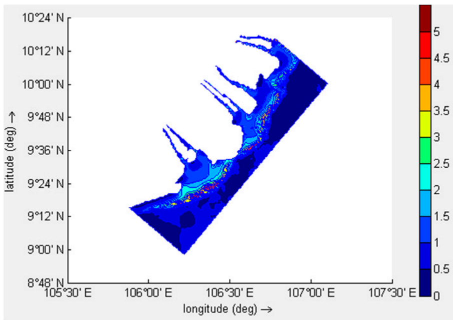

(**d**) Southwest wind in summer

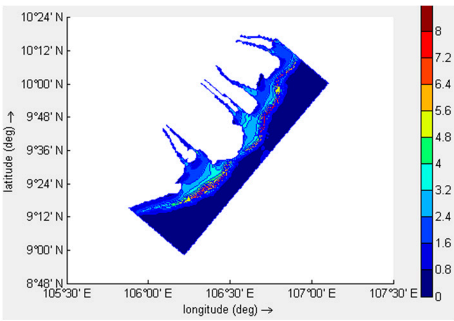

(**e**) Southeast wind in summer

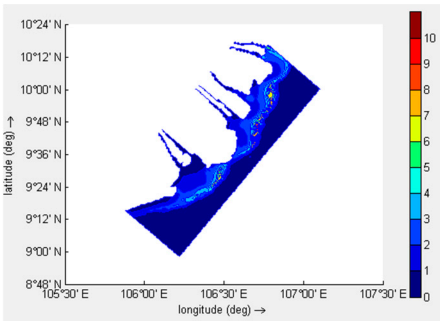

(**f**) Northeast wind in Winter

Figure 4. The shear stress on the bottom bed at the Mekong River Delta under no wind (**a**), northeast wind (**b**), northwest wind (**c**), southwest wind (**d**), southeast wind (**e**) in summer and northeast wind (**f**) in winter (Unit: Pa).

3.3. The Characteristics of Erosion and Disposition in the Yellow River Subaqueous Delta

Combining the distribution of shear stress on the bottom bed (Figure 5) and the distribution of water depth (Figure 6) in the Yellow River subaqueous delta, it is found that the subaqueous delta within 3 m of water depth is in a state of erosion and resuspension, and the transport range of sediment transported by Yellow River is mainly concentrated at this depth (Figure 7), resulting in the development of erosion residues and estuary dunes at the shallow water area of the Yellow River subaqueous delta [35]. With the strengthening of the winter monsoon, the erosion stress on the bottom bed of the seafloor has also increased correspondingly, causing the shear stress on the bottom bed in the shallow area of the delta with the depth <10 m to exceed the critical erosion stress (Figures 5f and 6a). Additionally, the lack of water and sediment transported by the Yellow River in the area with the depth is 3–10 m (Figure 7) may lead to erosion in the area.

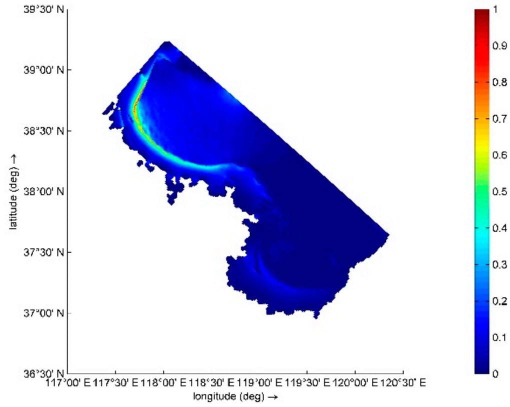

(**a**) No wind in summer.

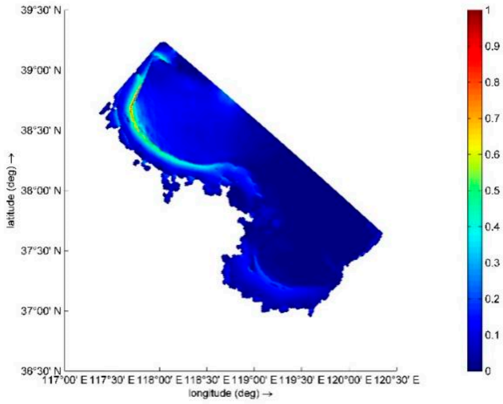

(**b**) Southwesterly wind in summer.

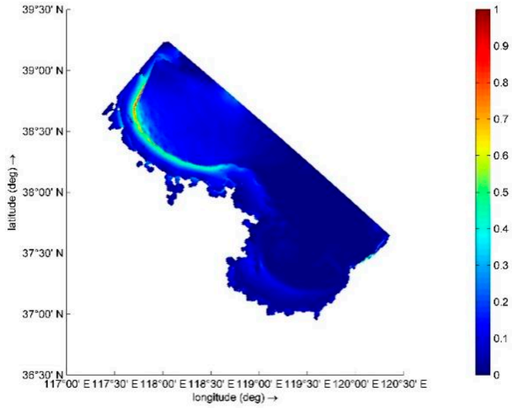

(**c**) Northwesterly wind in summer.

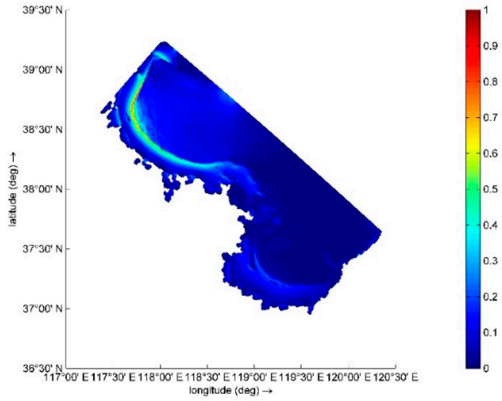

(**d**) Southwesterly wind in summer.

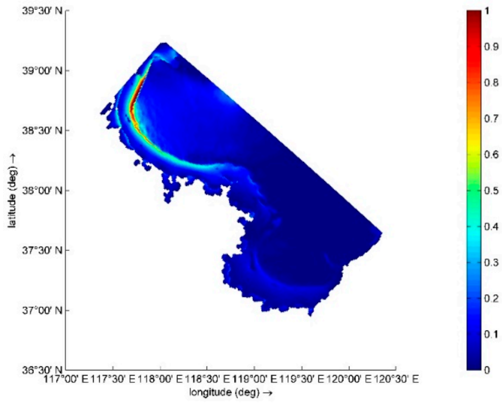

(**e**) Southeasterly wind in summer.

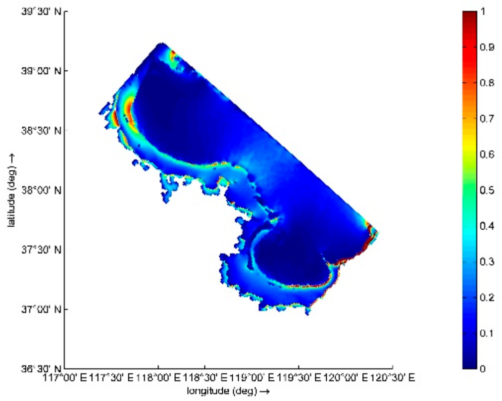

(**f**) Northeasterly wind in winter.

Figure 5. The shear stress on the bottom bed at the Yellow River Delta under no wind (**a**), northeast wind (**b**), northwest wind (**c**), southwest wind (**d**), southeast wind (**e**) in summer and northwest wind (**f**) in winter (Unit: Pa) [33].

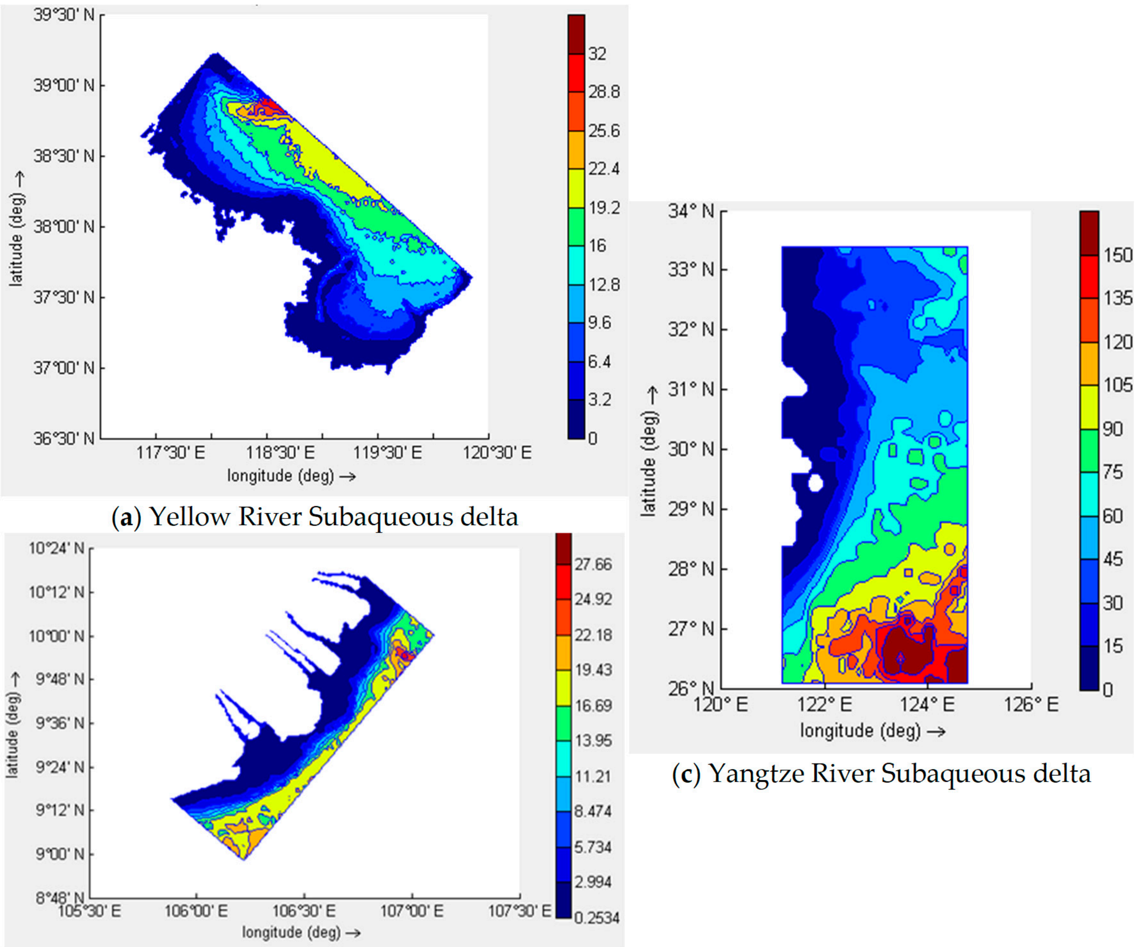

(**a**) Yellow River Subaqueous delta

(**b**) Mekong River Subaqueous delta

(**c**) Yangtze River Subaqueous delta

Figure 6. Water depth in Yellow River (**a**) Mekong River (**b**) and Yangtze River (**c**) Subaqueous delta (Unit: m).

3.4. The Characteristics of Erosion and Disposition in the Yangtze River Subaqueous Delta

In the area of the Yangtze River subaqueous delta (water depth: 0–15 m), the runoff and sediment fluxes in summer are much greater than that in winter. Under the influence of the monsoon, the sediment northward transportation is stronger than southward (Figure 8). Therefore, although the shear stress on the bottom bed in the northeast is stronger (Figure 9), but the erosion-type hazard geological types such as pits and gullies still occur at the northern Hangzhou Bay in the south of Yangtze Estuary [36]. It shows that the change in sediment transportation has a stronger influence on erosion and deposition in Yangtze River subaqueous delta than the shear stress on the bottom bed. The critical shear stress of the Yangtze River Delta is about 0.10 Pa [37], and the ratio (τ_t/τ_{crss}) of the total shear stress (τ_t) to the critical shear stress (τ_{crss}) is generally greater than 10, and the maximum value exceeds 30 in the Yangtze River subaqueous delta (water depth: 0–15 m) (Figures 4 and 6b). It can be inferred that the area in the Yangtze River subaqueous delta has been in a state of erosion throughout the year [38,39].

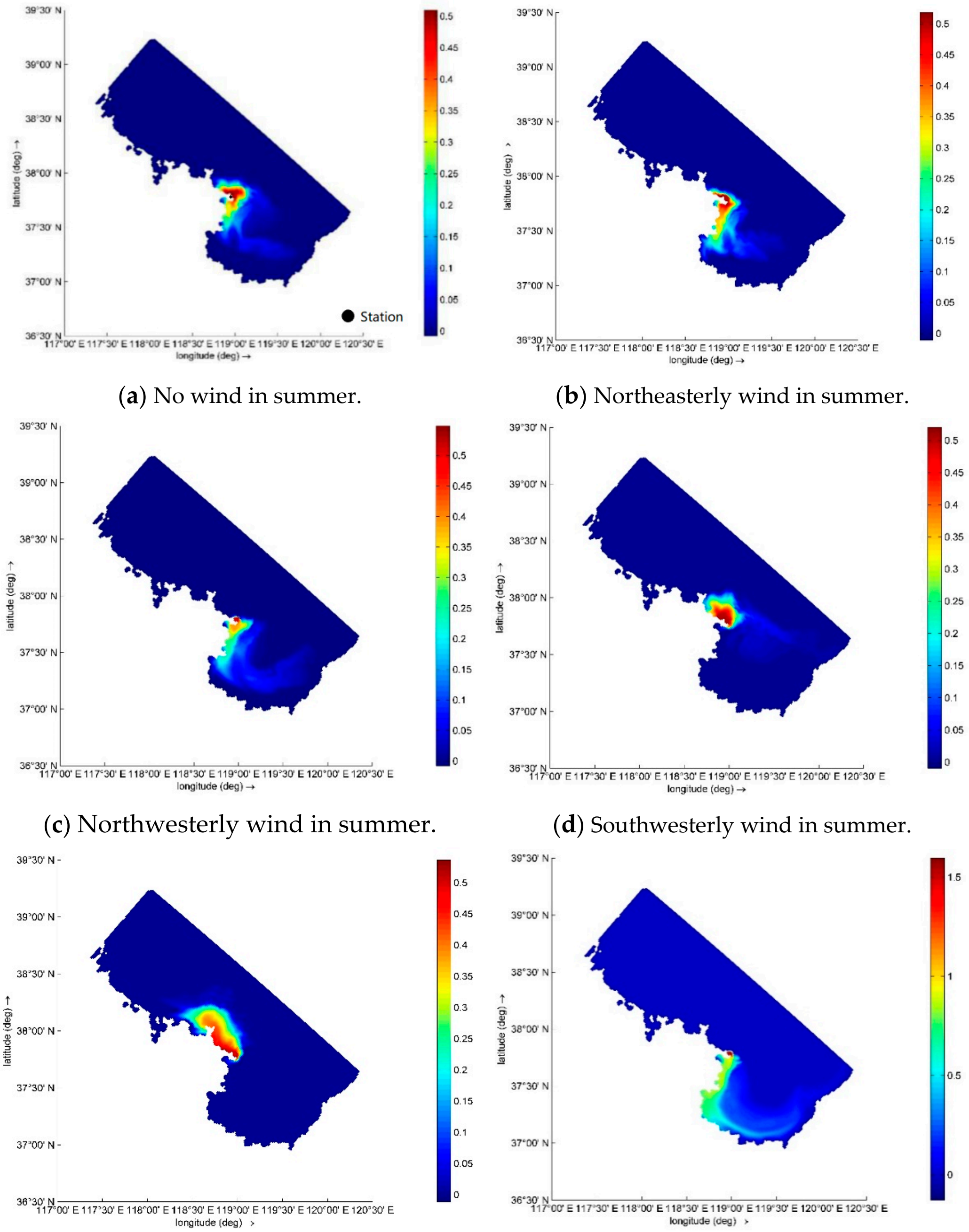

(**a**) No wind in summer. (**b**) Northeasterly wind in summer.

(**c**) Northwesterly wind in summer. (**d**) Southwesterly wind in summer.

(**e**) Southeasterly wind in summer. (**f**) Northwesterly wind in winter.

Figure 7. Suspended sediment transport at the Yellow River Delta under no wind (**a**), northeast wind (**b**), northwest wind (**c**), southwest wind (**d**), southeast wind (**e**) in summer and northwest wind (**f**) in winter (Unit: g/L) [30].

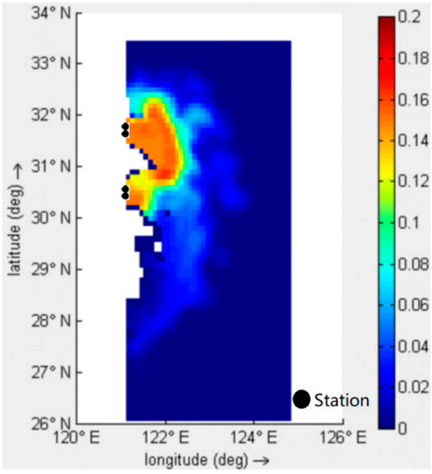

(**a**) No wind in Summer

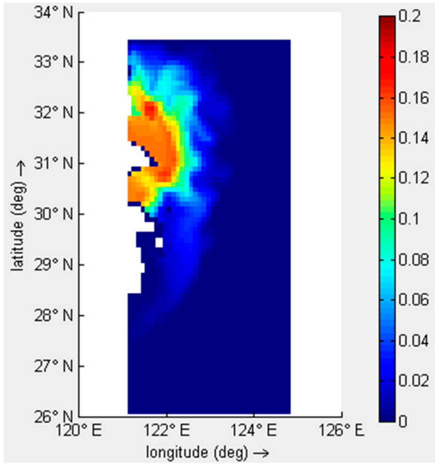

(**b**) East wind in summer

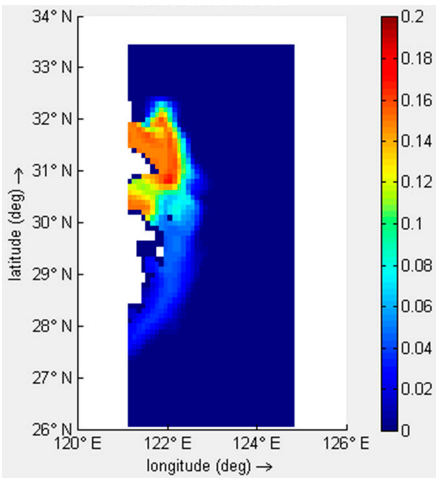

(**c**) North wind in summer

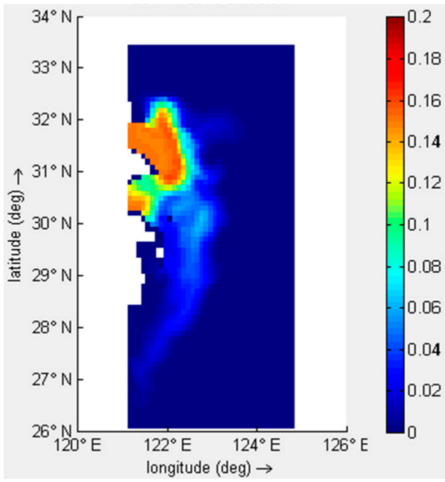

(**d**) West wind in summer

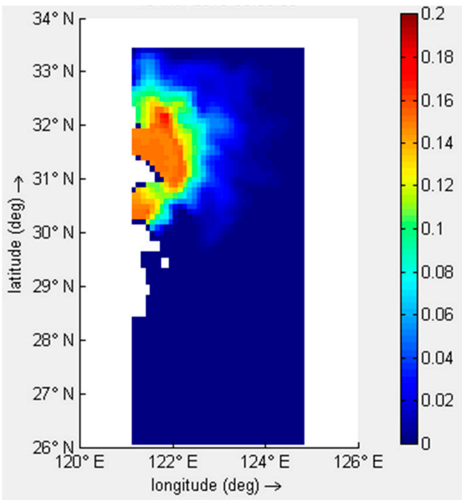

(**e**) South wind in summer

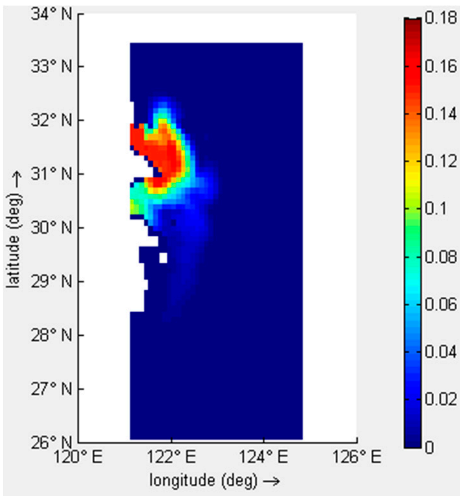

(**f**) North wind in Winter

Figure 8. Suspended sediment transport at the Yangtze River Delta under no wind (**a**), east wind (**b**), north wind (**c**), west wind (**d**), southeast wind (**e**) in summer and northwest wind (**f**) in winter (Unit: g/L) [30].

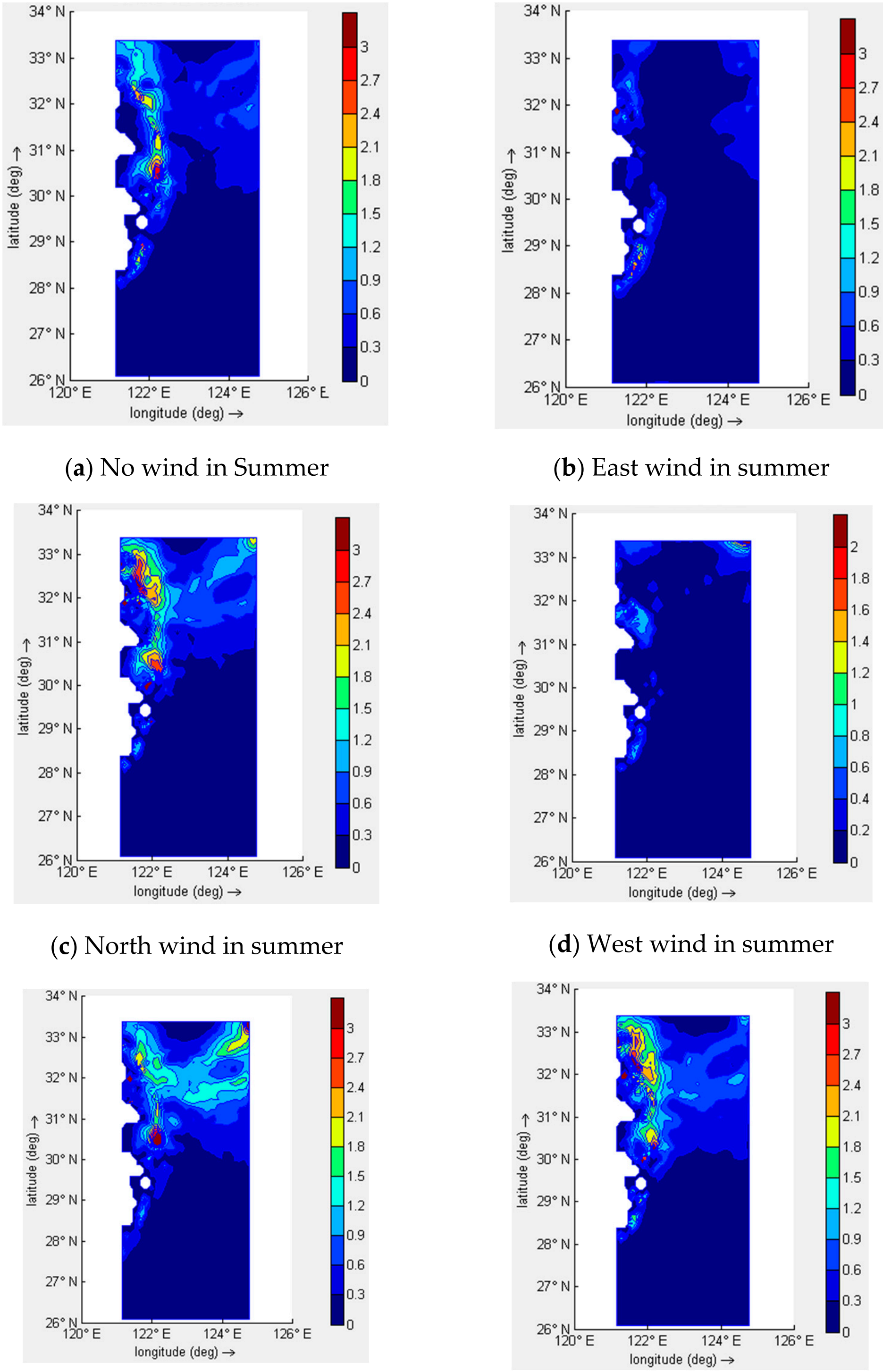

(**a**) No wind in Summer (**b**) East wind in summer

(**c**) North wind in summer (**d**) West wind in summer

(**e**) South wind in summer (**f**) North wind in Winter

Figure 9. The shear stress on the bottom bed at the Yangtze River Delta under no wind (**a**), east wind (**b**), north wind (**c**), west wind (**d**), south wind (**e**) in summer and north wind (**f**) in winter (Unit: Pa) [30].

3.5. The Characteristics of Erosion and Disposition in the Mekong River Subaqueous Delta

Due to the dam construction [40] and riverbed mining [19], the stability and erosion of the Mekong Delta, the third largest estuary in the world, have become a particularly important issue [41]. During 2014–2017, the channels in the Mekong Delta were severely erosive, with an erosive rate of -0.5 m/a, indicating that upstream development has caused large-scale morphological changes in the Mekong Delta [41]. To understand the erosion and accumulation of the Mekong River Delta, a field survey of the Mekong River subaqueous delta using sonar in 2014–2015 shows that the delta not only has a gradual erosion in land area, but also eroded in the subaqueous delta after 2005. Although there is a phenomenon of local accumulation near the estuary [12], its subaqueous delta generally appears to be eroded gradually, and under the action of coastal currents, the southern part of its delta is accompanied by the development of scour troughs [12,42].

The simulation results show that the transportation of water and sediment from the Mekong River is mainly controlled by wind direction. Under the influence of the monsoon, the southwest monsoon prevails in summer, so the sediment spreads northeast along the coast. Because the amount of water and sediment transported by Mekong River in winter is much less than that in summer, the runoff in winter is less than 1/6 of that in summer, so the transport range of the water and sediment in winter is much smaller than that in summer, the sediment transport is mainly concentrated near the estuary (Figures 2f and 3f). Additionally, the winter is dominated by the northeast monsoon that stronger than southwest monsoon in summer. It suggests that winter is the weakest season for the transport of suspended sediments in the Mekong River subaqueous delta, and it is also the season with the delta suffers the strongest erosion. According to the above reasons, the sediment transport in the Mekong River subaqueous delta mainly occurs in summer, and the southwest monsoon prevails in summer. Therefore, the main mode of the Mekong offshore transportation of suspended sediment under climatic conditions is transported northeast and southeast.

The results of in situ observations on the Mekong River subaqueous delta show that the SSC rises significantly when the current velocity near the bottom bed reaches 0.8 m/s [43]. It is assumed that the critical starting velocity is 0.8 m/s. Under the action, the critical shear stress is calculated to be about 0.20 Pa according to the flow-induced shear stress formula [44]. Combined with the distribution of shear stress on the bottom bed (Figure 4) and water depth distribution (Figure 9c), the ratio (τ_t/τ_{crss}) of total shear stress (τ_t) to critical shear stress (τ_{crss}) is generally greater than 10. Under the action of the southeast monsoon in summer and the northwest monsoon in winter, the ratio could even exceed 40 or 50. It can be inferred that the area in the Mekong River subaqueous delta has been in a state of erosion all year round [38,39].

3.6. Comparison of the Causes of Erosion and Deposition of Subaqueous Delta in the Yellow River, the Yangtze River and the Mekong River Delta

The erosion and accumulation process of estuarine deltas are mainly controlled by two main factors: sediment flux and hydrodynamic. The interaction process of the two factors makes the estuarine deltas' erosion and accumulation effects at different regions with different control factors have obvious differences. By comparing the distribution characteristics of the shear stress on the bottom bed produced by the action of wind and waves in the three typical East Asian estuary deltas such as the Yellow River, the Yangtze River and the Mekong River subaqueous delta (Figures 4, 5 and 9), and their topographic characteristics (Figure 6), it is found that hydrodynamic erosion driven by wind mainly occurs in shallow water areas.

For example, the critical erosion stress of the Yellow River Delta is about 0.30 Pa [45], combined with the distribution of shear stress on the bottom bed (Figure 5) and water depth distribution (Figure 6a), it is found that the Yellow River subaqueous delta with the water depth less than 3 m is in a state of erosion all year round. Additionally, the transport range of the sediment transported by Yellow River is mainly concentrated at this depth (Figure 7), resulting in the development of erosion residues and estuary sand dunes in the shallow water area in Yellow River subaqueous delta [35]. Additionally, the accelerate erosion process could induce deltaic ecosystem changes [46].

In addition, under the influence of human activities, the amount of sediment from the Yellow River, the Yangtze River and the Mekong River has decreased to varying degrees [3,4,47] cause the Yellow River subaqueous delta, which was originally a river-controlled delta, to turn into erosion from 2014 (Figure 10) [48]. As a river-tidal delta, the change in the amount of transport sediments in the Yangtze River subaqueous delta has a stronger impact on the erosion and accumulation of the subaqueous delta than the shear stress on the bottom bed, when the discharge of the sediment more than 6.0×10^8 t [8]. The decrease in the transportation of suspended sediments in the Yangtze River has led to the fact that its shoreline has ensured the stability under the influence of artificial shoreline reinforcement, but its subaqueous delta has been eroded all year round.

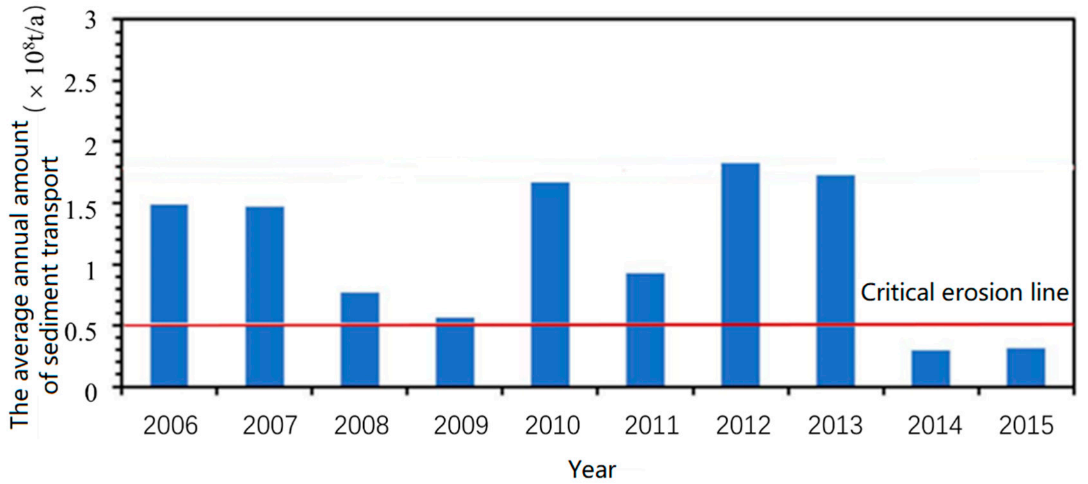

Figure 10. Annual erosion and deposition at the Yellow River's subaqueous delta (data from the Yangtze River Sediment Bulletin).

The shear stress on the bottom of the Mekong River subaqueous delta is not only stronger than that of the Yangtze River Delta (Figures 2 and 8), and the amount of sediment only 1/3 of that transported by the Yangtze River. Additionally, the shoreline of Mekong Delta is lack of protection [13] caused its shoreline to be eroded [41]. However, because the Mekong River's runoff and sediment fluxes in summer is much larger than in winter, under the influence of the monsoon, the sediment transports to northward are more than southward, so the erosion intensity of the northern part in the Mekong River subaqueous delta is relatively weaker [12]. The southern part suffered strong erosion and developed erosion troughs [12,49], the degree of erosion gradually weakened from south to north. The coastal protection structures should be used to decrease the erosion in Mekong River delta include revetments, geotubes, t-shaped bamboo fences, Pile-rock breakwaters, Busadco's breakwaters, Semi-Circular breakwaters, Hollow triangle breakwaters and multiple lines of defense (a green infrastructure inspired nature-based solution) [50].

According to the simulation results, the sediment transport in the three deltas is mainly concentrated in summer, which may be due to the monsoon climate with more rain in summer and less rain in winter, which causes the river runoff to be mainly concentrated in summer. In addition, the southern part of the Asian monsoon climate zone is close to the ocean, and the southerly wind prevails in summer, causing the sediment transported by river mainly to the southern part of its subaqueous delta (Figures 3, 7 and 8). Under the action of the Coriolis force, the shear stress on the southern bed of the three subaqueous deltas is also larger (Figures 4, 5 and 9). Therefore, when the subaqueous delta is greatly affected by the incoming sediment, the deposition of suspended sediment is stronger than the hydrodynamic erosion, and deposition occurs in the southern part of the subaqueous delta. Currently, the delta is a river-controlled delta. Conversely, when the subaqueous delta is greatly affected by tides and waves, the hydrodynamic erosion is stronger than the deposition of suspended sediment, and the delta is a tide-controlled or wave-controlled delta at this time. The erosion and deposition patterns also confirm this view, that the patterns present “northern erosion and south accumulation” in Yellow River delta and the degree of erosion gradually weakened from south to north in Mekong River delta.

Additionally, the driving force of sediment transport and delta bed erosion are both hydrodynamic. Comparing the sediment transport range and the distribution range of bottom shear stress in the simulation results [19], it is found that the two are basically consistent (Figures 3–5 and 7–9). It is further deduced that if the hydrodynamic forces driving the resuspended sediment transport are consistent with the seabed erosion. It is only necessary to analyze the erosion and deposition in the main transport area of the resuspended sediment, the changes in the properties of the entire subaqueous delta can be recognized. This assumption, if true, will greatly reduce the workload of subaqueous delta erosion and deposition studies.

3.7. Error Analysis

Due to insufficient consideration of hydrodynamic erosion on sediments and the source of sediments in the simulation calculation, the simulation results can only conduct a qualitative comparative study on the causes of erosion in subaqueous deltas. For example, the wind speed used in the calculation is the monthly average wind speed, which cannot accurately simulate the instantaneous shear stress on the bottom bed. In addition, the plants on the delta may also affect the hydrodynamic erosion of the delta. For example, the large healthy marginal mangrove belt on the Mekong Delta can effectively protect the coastline [13]. Moreover, suspended sediments produced by human activities and delta erosion will also affect the erosion and accumulation of subaqueous deltas [13,41]. For example, since the 1950s, continuous construction and reinforcement of the eroded banks in the Yangtze River Delta (such as the construction of the seawall and T-shaped dam) have made the bank slopes generally stabilized [27], while increasing the amount of suspended sediments in the subaqueous delta led to the accumulation of the north channel [22]. Additionally, the study only focused on the redistribution of sediment in the subaqueous delta under the action of marine forcing, without considering the estuarine processes of vertical mixing. These problems need to be supplemented and improved in future work, in order to achieve rapid acquisition of the erosion and accumulation situation in the estuary subaqueous delta by combining the wave, wind speed, and wind direction data obtained by the satellite and the runoff and sediment fluxes obtained by the hydrological station through the numerical simulation method.

4. Conclusions

The three typical East Asian estuaries—the Yellow River, the Yangtze River and the Mekong River, are all distributed in the monsoon climate zone. The Delft 3D numerical simulation method is used to simulate and compare the erosion and accumulation effects of the estuary delta. It is found that the combined effect of transport of sediment transported by rivers and hydrodynamic at the same depth is the main control factors that affect the sediment erosion and accumulation process in the estuary delta. The combined effect of the transport of sediment, wind and waves shapes the erosion and accumulation topography of different large estuarine deltas in different regions and different climate backgrounds.

The sediment transported from the Yangtze River and the Mekong River is mainly concentrated in summer. The Yangtze River Delta has a relatively large supply of sediment about three times that of the Mekong River. However, different areas of erosion or accumulation have occurred under the artificial reinforcement of the shoreline (increasing the amount of sediment into the sea). In general, the Yangtze River subaqueous delta presents the "northern accumulation and south erosion" model. The Mekong River transport less amount of sediment. Additionally, it directly discharges into the open sea, the hydrodynamic effect is stronger. These induced the subaqueous delta as a whole is erosion, and the erosion modes present "strong in the south and weak in the north" pattern.

Human activities, especially the construction of dams in the upstream, have severely reduced the amount of water and sediment transported by large East Asia rivers, and caused the erosion to strengthen in the East Asia subaqueous delta. For example, in recent years, the Yellow River and the Yangtze River subaqueous delta have received less sediment. The Yellow River delta has experienced varying degrees of erosion, and the erosion of the subaqueous delta and the transport range of sediment transported by Yellow River are mainly concentrated in the area within 3 m of water depth, but its accumulation landforms concentrate in the direction of Coriolis forces presents it is still dominated by the transport of sediment, which is originally a river-controlled delta. However, the decrease in the transportation amount of suspended sediments in the Yangtze River has led to the subaqueous delta (water depth: 0–15 m) is in a state of erosion all year round, and the transported sediment has a weaker impact on the erosion and accumulation of the subaqueous delta than the shear stress on bottom bed presents the river delta may be changed from a river-tidal delta to a delta controlled by hydrodynamic.

The construction of coastal projects also affects the erosion and accumulation of the subaqueous delta, the Yangtze River Delta has ensured the stability of its shoreline and increased the amount of suspended sediments in the subaqueous delta under the influence of artificial shoreline reinforcement, but its estuary sand barriers and subaqueous deltas have experienced varying degrees of erosion. However, in the Mekong River subaqueous delta, because of lack of artificial shoreline protection, and the ratio (τ_t/τ_{crss}) of the total shear stress (τ_t) to the critical shear stress (τ_{crss}) is generally greater than 10, under the action of the southeast monsoon in summer and the northwest monsoon in winter, the ratio can even exceed 40 or even 50. Therefore, erosion generally occurs in the range of its shoreline and subaqueous delta (water depth 0–15 m), and the erosion modes present "strong in the south and weak in the north" pattern, this shows that the erosion and accumulation of the Mekong River subaqueous delta is still controlled by hydrodynamic.

Based on the above conclusions, we conclude that the transport of resuspended sediment and sea bed erosion are controlled by hydrodynamics. Therefore, analyzing the erosion and deposition within the transport range of resuspended sediment, the changes in the properties of the entire subaqueous delta could be recognized. For example, although the hydrodynamic conditions and climatic environment of the three deltas are different, their sediment transport is concentrated in summer and mainly transported to the south under the effect of monsoon. At the same time, due to the Coriolis force effects and prevailed winter monsoons, the southern bed of the northern hemisphere estuary delta is also affected by stronger shear stress, so the southern part of the river controlled subaqueous delta is dominated by deposition, while the southern part of the hydraulic controlled delta is dominated by erosion. This rule is also helpful to analyze whether the change of river sediment will lead to the change of delta type under human influence.

Author Contributions: Software, J.P.L.; data curation, B.L.; writing—original draft preparation, B.L.; writing—review and editing, B.L.; funding acquisition, B.L.; supervision, Y.J. All authors have read and agreed to the published version of the manuscript.

Funding: This research was funded by "National Natural Science Foundation of China" (42107157), "the Fundamental Research Funds for the Central Universities, SCUT" (22CX01004A-8, 21CX06016A).

Data Availability Statement: The data presented in this study are available on request from the corresponding author. The data are not publicly available due to the data takes up too much space.

Acknowledgments: Special thanks go to the Ocean University of China for the joint training MSc programs and NC State University giving me a visiting scholar chance.

Conflicts of Interest: The authors declare no conflict of interest.

References

1. Wang, H.; Sun, F. Variability of annual sediment load and runoff in the Yellow River for the last 100 years (1919–2018). *Sci. Total Environ.* **2021**, *758*, 143715. [CrossRef] [PubMed]
2. Binh, D.V.; Kantoush, S.; Sumi, T. Changes to long-term discharge and sediment loads in the Vietnamese Mekong Delta caused by upstream dams. *Geomorphology* **2020**, *353*, 107011. [CrossRef]

3. Lu, J.; Qiao, F.L.; Wang, X.H.; Teng, Y.; Jung, K.T.; Liu, Y.G. Modeling the Yellow River sediment flux and its deposition patterns under climatological conditions. *Ocean. Dyn.* **2013**, *63*, 709–722. [CrossRef]
4. Zhang, R.; Wang, Y.; Pan, S. Variations of Suspended Sediment Concentrations and Loads into the Estuary Area from Yangtze River in Recent 50 Years. *Mar. Sci. Bull.* **2008**, *27*, 1–9. (In Chinese)
5. Stefanidis, S.; Alexandridis, V.; Ghosal, K. Assessment of Water-Induced Soil Erosion as a Threat to Natura 2000 Protected Areas in Crete Island. Greece. *Sustainability* **2022**, *14*, 2738. [CrossRef]
6. Mashhadi, A.; Jafari, R. Mapping and quantitative identification of sensitive regions to land degradation in south of Isfahan province using modified MEDALUS model. *J. Geogr. Environ. Hazards* **2022**, *11*, 1.
7. Jiang, C.; Pan, S.Q.; Chen, S.L. Recent morphological changes of the Yellow River (Huanghe) submerged delta: Causes and environmental implications. *Geomorphology* **2017**, *293 Pt A*, 93–107. [CrossRef]
8. Jia, J.; Gao, J.; Cai, T.; Li, Y.; Yang, Y.; Wang, Y.P.; Xia, X.; Li, J.; Wang, A.; Gao, S. Sediment accumulation and retention of the Changjiang (Yangtze River) subaqueous delta and its distal muds over the last century. *Mar. Geol.* **2018**, *401*, 2–16. [CrossRef]
9. Luang, H.L.; Ding, P.X.; Wang, Z.B.; Ge, J.Z. Process-based morphodynamic modeling of the Yangtze Estuary at a decadal timescale: Controls on estuarine evolution and future trends. *Geomorphology* **2017**, *290*, 347–364. [CrossRef]
10. DeMaster, D.J.; Liu, J.P.; Eidam, E.; Nittrouer, C.A.; Nguyen, T.T. Determining rates of sediment accumulation on the Mekong shelf: Timescales, steady-state assumptions, and radiochemical tracers. *Cont. Shelf Res.* **2017**, *147*, 182–196. [CrossRef]
11. Xue, Z.; He, R.; Liu, J.P.; Warner, J.C. Modeling transport and deposition of the Mekong River sediment. *Cont. Shelf Res.* **2012**, *37*, 66–78. [CrossRef]
12. Liu, J.P.; DeMaster, D.J.; Nguyen, T.T.; Saito, Y.; Nguyen, V.L.; Ta, T.K.O.; Li, X. Stratigraphic formation of the Mekong River Delta and its recent shoreline changes. *Oceanography* **2017**, *30*, 72–83. [CrossRef]
13. Besset, M.; Gratiot, N.; Anthony, E.J.; Bouchette, F.; Goichot, M.; Marchesiello, P. Mangroves and shoreline erosion in the Mekong River delta, Vietnam. *Estuar. Coast. Shelf Sci.* **2019**, *226*, 106–263. [CrossRef]
14. Fricke, A.T.; Nittrouer, C.A.; Ogston, A.S.; Vo-Luong, H.P. Asymmetric progradation of a coastal mangrove forest controlled by combined fluvial and marine in fluence, Cù Lao Dung, Vietnam. *Cont. Shelf Res.* **2017**, *147*, 78–90. [CrossRef]
15. Mullarney, J.C.; Henderson, S.M.; Reyns, J.A.H.; Bouchette, F.; Goichot, M.; Marchesiello, P. Spatially varying drag within a wave-exposed mangrove forest and on the adjacent tidal flat. *Cont. Shelf Res.* **2017**, *147*, 102–113. [CrossRef]
16. Henderson, S.M.; Norris, B.K.; Mullarney, J.C.; Bryan, K.R. Wave-frequency flows within a near-bed vegetation canopy. *Cont. Shelf Res.* **2017**, *147*, 91–101. [CrossRef]
17. Meng, X.M.; Jia, Y.G.; Shan, H.X.; Yang, Z.N.; Zheng, J.W. An experimental study on erodibility of inter tidal sediments in the Yellow River delta. *Int. J. Sediment Res.* **2012**, *27*, 240–249. [CrossRef]
18. Fan, H.; Huang, H.; Zeng, T.Q.; Wang, K.R. River mouth bar formation, riverbed aggradation and channel migration in the modern Huanghe (Yellow) River delta, China. *Geomorphology* **2006**, *74*, 124–136. [CrossRef]
19. Burchard, H.; Schuttelaars, H.M.; Ralston, D.K. Sediment trapping in estuaries. *Annu. Rev. Mar. Sci.* **2018**, *10*, 371–395. [CrossRef]
20. Nakanowatari, T.; Nakamura, T.; Mitsudera, H.; Nishioka, J.; Kuroda, H.; Uchimoto, K. Interannual to decadal variability of phosphate in the Oyashio region: Roles of wind-driven ocean current and tidally induced vertical mixing in the Sea of Okhotsk. *Prog. Oceanogr.* **2021**, *197*, 102615. [CrossRef]
21. Gong, W.; Zhang, G.; Yuana, L.; Zhu, L.; Zhang, H. Effects of swell waves on the dynamics of the estuarine turbidity maximum in an idealized convergent partially mixed estuary. *J. Mar. Syst.* **2022**, *235*, 103784. [CrossRef]
22. Zheng, S.; Cheng, H.; Lv, J.; Li, Z.; Zhou, L. Morphological evolution of estuarine channels influenced by multiple anthropogenic stresses: A case study of the North Channel, Yangtze estuary, China. *Estuar. Coast. Shelf Sci.* **2021**, *249*, 107075. [CrossRef]
23. Tamura, T.; Nguyen, V.L.; Ta, T.K.O.; Bateman, M.D.; Gugliotta, M.; Anthony, E.J.; Nakashima, R.; Saito, Y. Long-term sediment decline causes ongoing shrinkage of the Mekong megadelta, Vietnam. *Sci. Rep.* **2020**, *10*, 8085. [CrossRef] [PubMed]
24. Zhou, L.; Liu, J.; Saito, Y.; Diao, S.B.; Gao, M.S.; Qiu, J.D.; Xu, C.L.; He, L.L.; Ye, S.Y. Sediment budget of the Yellow River delta during 1959–2012, estimated from morphological changes and accumulation rates. *Mar. Geol.* **2020**, *430*, 106363. [CrossRef]
25. Fu, R.; Yu, Z.; Jin, M.; Fang, W. Variation trend of runoff and sediment load in Yangtze River. *J. Hydraul. Eng.* **2003**, *11*, 23–29. (In Chinese)
26. He, D. Analysis of hydrological characteristics in Lancing-Mekong River. *Yunnan Geogr. Environ. Res.* **1995**, *7*, 58–74. (In Chinese)
27. Qiu, C.Y.; Li, X.; Liu, S.A.; Chen, D. Monitoring tidal flats in the Yangtze River Delta using Landsat images. *J. Geo-Inf. Sci.* **2019**, *21*, 269–278. (In Chinese)
28. Wolanski, E.; Huan, N.N.; Dao, L.T.; Nhan, N.H.; Thuyc, N.N. Fine-sediment dynamics in the Mekong River estuary, Vietnam. *Estuar. Coast. Shelf Sci.* **1996**, *43*, 565–582. [CrossRef]
29. Xue, L.; Galloway, W.E. Fan-delta, braid delta and the classification of delta system. *Acta Geol. Sin.* **1991**, *65*, 141–153. (In Chinese)
30. Xu, S.; Chen, Z. Similarity and discrepancy of major delta processes on eastern coast of China. *Acta Geogr. Sin.* **1995**, *50*, 481–490. (In Chinese)
31. Li, B.; Liu, J.P.; Jia, Y.G. Comparison of the Causes of Erosion–Deposition between Yellow River, Yangtze River, and Mekong River Subaqueous Delta l: Model Building. *Water* **2022**, *14*, 3208. [CrossRef]
32. Galloway, W.E. Process Framework for Describing the Morphologic and Stratigraphic Evolution of Deltaic Depositional Systems. In *Deltas: Models for Exploration*; Houston Geological Society: Houston, TX, USA, 1975; pp. 87–98.

33. Wang, J.; Li, J.; Li, R.; Liu, H. Seasonal Characteristics Analysis of the Sea Surface Wind Field in the South China Sea. *Sci. Technol. Inf.* **2014**, *03*, 197–200. (In Chinese)
34. Szczuciński, W.; Jagodziński, R.; Hanebuth, T.J.J.; Stattegger, K.; Wetzel, A.; Mitrega, M.; Unverricht, D. Modern sedimentation and sediment dispersal pattern on the continental shelf off the Mekong River delta, South China Sea. *Glob. Planet. Chang.* **2013**, *110*, 195–213. [CrossRef]
35. Li, P. Mechanism and Division of Typical Geological Hazards on the Surface and Shall of Seabed of the Yellow River Delta Offshore. Ph.D. Thesis, Ocean University of China, Qingdao, China, 2015. (In Chinese).
36. Guo, X.; Yan, X.; Zheng, S.; Wang, H.M.; Yin, P. Characteristics of high-resolution subaqueous micro-topography in the Jinshan Deep Trough and its implications for riverbed deformation, Hangzhou Bay, China. *Estuar. Coast. Shelf Sci.* **2021**, *250*, 107147. [CrossRef]
37. Yang, H.F.; Yang, S.L.; Xu, K.H.; Wu, H.; Shi, B.W.; Zhu, Q.; Zhang, W.X.; Yang, Z. Erosion potential of the Yangtze Delta under sediment starvation and climate change. *Sci. Rep.* **2017**, *7*, 10535. [CrossRef]
38. Li, B.; Jia, Y.; Zhang, Y.; Shan, H. Study on processes of seabed in the Yellow River Delta. *J. Sediment Res.* **2020**, *45*, 16–22. (In Chinese)
39. Aghsaee, P.; Boegman, L. Experimental investigation of sediment resuspension beneath internal solitary waves of depression. *J. Geophys. Res. Ocean.* **2015**, *120*, 3301–3314. [CrossRef]
40. Kondolf, G.M.; Rubin, Z.K.; Minear, J.T. Dams on the Mekong: Cumulative sediment starvation. *Water Resour. Res.* **2014**, *50*, 5158–5169. [CrossRef]
41. Anthony, E.J.; Brunier, G.; Besset, M.; Goichot, M.; Dussouillez, P.; Nguyen, V.L. Linking rapid erosion of the Mekong River delta to human activities. *Sci. Rep.* **2015**, *5*, 14745. [CrossRef]
42. Liu, J.P.; De Master, D.J.; Nittrouer, C.A.; Eidam, E.F.; Nguyen, T.T. A seismic study of the Mekong subaqueous delta: Proximal versus distal accumulation. *Cont. Shelf Res.* **2017**, *147*, 197–212. [CrossRef]
43. Unverricht, D.; Nguyen, T.C.; Heinrich, C.; Szczucinski, W.; Lahajnar, N.; Stattegger, K. Suspended sediment dynamics during the inter-monsoon season in the subaqueous Mekong Delta and adjacent shelf, southern Vietnam. *J. Asian Earth Sci.* **2014**, *79*, 509–519. [CrossRef]
44. Lund-Hansen, C.; Valeur, J.; Pejrup, M.; Jensen, A. Sediment fluxes, re-suspension and accumulation rates at two wind-exposed coastal sites and in a sheltered Bay. *Estuar. Coast. Shelf Sci.* **1997**, *44*, 521–531. [CrossRef]
45. Li, B.; Jia, Y.; Liu, J.P.; Su, J.F.; Liu, X.L.; Wen, M.Z. The controlling factors of high suspended sediment concentration in the intertidal flat off the Huanghe River Estuary. *Acta Oceanol. Sin.* **2020**, *39*, 96–106. [CrossRef]
46. Zhao, H.; Lin, Y.; Delang, C.O.; Ma, Y.; Zhou, J.; He, H.M. Contribution of soil erosion to the evolution of the plateau-plain-delta system in the Yellow River basin over the past 10,000 years. *Palaeogeogr. Palaeoclimatol. Palaeoecol.* **2022**, *601*, 111133. [CrossRef]
47. Peng, J.; Chen, S. The Variation Process of Water and Sediment and Its Effect on the Yellow River Delta over the Six Decades. *Acta Geogr. Sin.* **2009**, *11*, 1353–1362. (In Chinese)
48. Bi, N.S.; Wang, H.J.; Yang, Z.S. Recent changes in the erosion–accretion patterns of the active Huanghe (Yellow River) delta lobe caused by human activities. *Cont. Shelf Res.* **2017**, *90*, 70–78. [CrossRef]
49. Anthony, E.J.; Dussouillez, P.; Dolique, F.; Besset, M.; Brunier, G.; Nguyen, V.L.; Goichot, M. Morphodynamics of an eroding beach and foredune in the Mekong River delta: Implications for deltaic shoreline change. *Cont. Shelf Res.* **2017**, *147*, 155–164. [CrossRef]
50. Xuan, T.L.; Ba, H.T.; Vo Quoc Thanh, V.Q.; Wright, D.P.; Tanim, A.H.; Anh, D.T. Evaluation of coastal protection strategies and proposing multiple lines of defense under climate change in the Mekong Delta for sustainable shoreline protection. *Ocean. Coast. Manag.* **2022**, *228*, 106301. [CrossRef]